LBL-11553 c.2
Preprint

Lawrence Berkeley Laboratory
UNIVERSITY OF CALIFORNIA

Materials & Molecular Research Division

Submitted to the Journal of Vacuum Science and Technology

DESIGN OF A MOLECULAR BEAM SURFACE SCATTERING APPARATUS FOR VELOCITY AND ANGULAR DISTRIBUTION MEASUREMENTS

S.T. Ceyer, W.J. Siekhaus, and G.A. Somorjai

November 1980

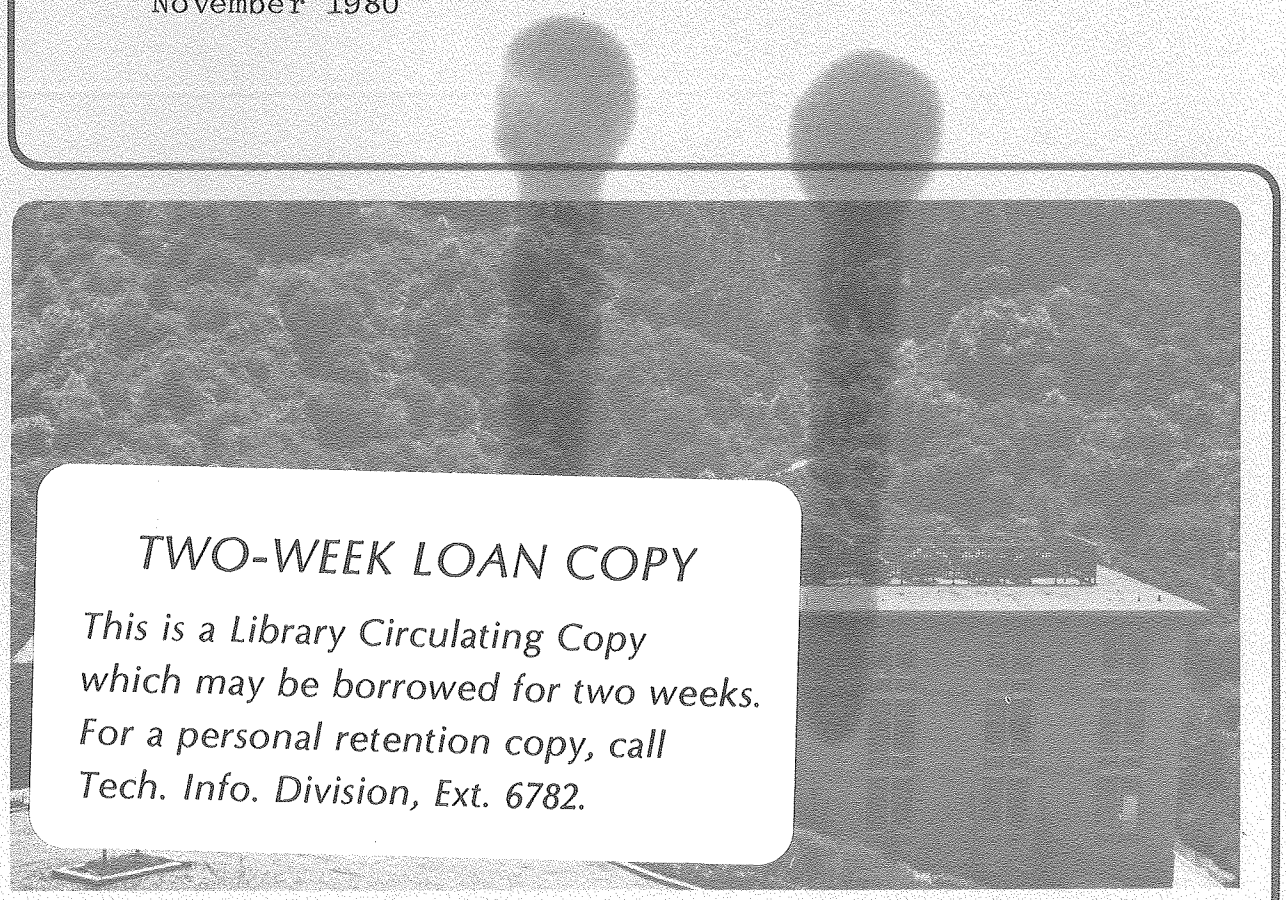

Prepared for the U.S. Department of Energy under Contract W-7405-ENG-48

DISCLAIMER

DESIGN OF A MOLECULAR BEAM SURFACE SCATTERING APPARATUS FOR VELOCITY AND ANGULAR DISTRIBUTION MEASUREMENTS

S.T. Ceyer,[1] W.J. Siekhaus,[2] and G.A. Somorjai

Materials and Molecular Research Division, Lawrence Berkeley Laboratory, and Department of Chemistry, University of California, Berkeley, California 94720

Abstract

A molecular beam surface scattering apparatus designed for the study of corrosion and catalytic surface reactions is described. The apparatus incorporates two molecular or atomic beams aimed at a surface characterized by low energy electron diffraction (LEED) and Auger electron spectroscopy (AES), a rotatable, differentially pumped quadrupole mass spectrometer, and a versatile manipulator. Angular distributions and energy distributions as a funcion of angle and independent of the surface residence time can be measured. Typical data for the oxidation of deuterium to D_2O on a Pt(111) crystal surface are presented.

[1]Present address: National Bureau of Standards, Washington, DC 20234.

[2]Present address: Lawrence Livermore Laboratory, Livermore, CA 94550.

This work was supported by the Director, Office of Energy Research, Office of Basic Energy Sciences, Materials Sciences Division of the U.S. Department of Energy under Contract No. W-7405-ENG-48.

Introduction

A microscopic description of the trajectory of a gaseous atom or molecule near the surface of a solid is the ultimate aim in understanding the gas-solid interaction. Of particular interest to a chemist are the mechanisms for desorption and energy disposal after a strong chemical interaction with the surface. The spatial and energy distributions of molecules scattered or desorbed from the surface are determined by the dynamics of this interaction. Measurements of these distributions can yield information regarding the degree of energy exchange per collision between a gas molecule and the surface, the nature of the potential energy surface of a gas-solid or catalytic chemical reaction, and the energetics of a surface chemical reaction.

The experimental schemes for measuring the spatial or angular distribution and energy distribution of molecules scattered or desorbed from a surface as well as the surface residence time distribution and primary product distribution of a surface chemical reaction are shown in Figures 1a and 1b. Spatially and energetically well defined beams of atoms or molecules strike the surface and the species that are scattered or desorbed from the surface are detected by a quadrupole mass spectrometer. The angular distributions are measured by rotating the mass spectrometer around the surface. The incident beam is modulated mechanically in an experiment measuring surface residence times (Fig.1a), whereas the scattered beam is modulated in an experiment measuring the velocity distribution of the beam after interaction with the surface (Fig. 1b). The surface residence time distribution or the time-of-flight distribution (subsequently transformed to a velocity and then energy distribution) results from a measurement of the time delay between a reference signal from the chopper which modulates the beam and the arrival of the molecules at the detector. The mass spectrometer detector, in the line of sight of the surface, enables the primary product distribution of a surface chemical reaction to be determined unambiguously.

The purpose of this paper is to describe an apparatus recently built which has been designed to measure these distributions.[1] A schematic of the apparatus is shown in Fig.2. The next two sections discuss the

design considerations and the essential parts of the working instrument. The last section presents some experimental results of reactive scattering obtained in this system. It is hoped that the detailed description of the instrument aids in the wide utilization of this technology for studies of surface chemical reactions.

Design Considerations

There are two concerns which dominate the design considerations: the maximization of the product signal relative to the background intensity at the mass number of interest, and the maintenance of ultrahigh vacuum in the sample surface chamber. The maximization of the product signal relative to the background intensity is accomplished primarily by differentially pumping the beam source and the detector. This arrangement allows the beam source to operate at high pressures so that the flux of molecules in the beam incident on the surface is much higher (10^4:1) than the flux of molecules incident on the surface from the background gas in the main scattering chamber. In addition, since the flux incident on the sample surface at a distance r decreases with respect to the flux leaving the source as $1/r^2$, the distance between the source and the surface must be minimized (about 3"). However, the detector must be positioned at a distance from the surface (6"), which is large compared to the ionizer length of the quadrupole mass spectrometer (0.25"), in order to achieve sufficient velocity resolution (8%). Because the detector is far from the surface, product ionization probabilities are small and product angular distributions broad, the detector is doubly differentially pumped to reduce the contribution from the main chamber to the background product signal. The background product signal in the main chamber arises from the residual part of the product angular distribution and from product produced on the walls or in the pumps of the main chamber. It is also necessary to have a high pumping speed in the main chamber to minimize this background contribution at the detector. Another major source of background signal at the detector is from the beam load. This is most effectively solved by allowing the beam to pass through the ionizer and mass spectrometer chamber before

it collides with a wall. Lack of space prevented this implementation. A high pumping speed in the detector chamber also minimizes the background due to the beam load and outgassing, mainly H_2, from the bulk of the stainless steel walls. The outgassing rate of the walls of the detector chamber is reduced by baking the stainless steel chamber in a vacuum over at high temperature. This procedure reduces the outgassing rate of stainless steel by two orders of magnitude.[2]

The maintenance of very low pressures in the main scattering chamber in addition to the detector chamber is a necessary condition for obtaining a clean, well characterized surface and for the use of electron spectroscopies for surface analysis. All materials, including the chopper motor for time-of-flight measurements used in the construction of the main chamber, must be ultrahigh vacuum compatible (low outgassing rates and bakeable to 250°C). Placement of the motor in the main chamber allows the modulation of the scattered product of a surface chemical reaction. Modulation of the scattered beam, rather than modulation of the incident beam in a time-of-flight experiment, precludes the measurement of an additional dealy time due to the residence time of the surface reaction. The residence times for surface reactions have been shown to be as long as several milliseconds.[3]

With two separate, differentially pumped beam sources, surface reactions involving two reactive incident beams, H+D atom recombination for example, can be investigated. In addition, it is prefereable that a line of sight through the beam sources and detector exists to facilitate the alignment of the sample surface so that the plane of the surface is perpendicular to the plane determined by the incident beam and the detector viewing angle. Although the apparatus can be designed such that the beam sources and detector are aligned upon assembly, the sample surfaces of various sizes are interchanged often and are subject to slight warpage during heating cycles. The alignment adjustments of the surface are accomplished from the outside of the vacuum by a manipulator which translates, rotates the sample surface around a perpendicular and parallel axis, and tilts the sample surface.

Description of the Apparatus

Beam Sources and Chambers

Two independent and twice differentially pumped beam sources are aimed at the center line of the cylindrical main chamber which lies in the plane determined by the two incident beams. The beams form a 30° angle to each other. The two sources and two source buffer chambers formed one welded unit which was fitted and welded into a slot cut into the cylindrical main chamber, as shown in Fig.3. This design minimizes the distance between the beam source and the sample surface, and most closely packs the four diffusion pumps. Presently, the source and source buffer chambers are each pumped by a liquid nitrogen trapped 6" diffusion pump. The beam source flanges have rectangular cross sections as opposed to circular ones to maximize the angular range of the detector rotation. One of the beams is modulated in the buffer chamber by a tuning fork chopper of fixed frequency or by a motor driven chopper wheel of variable frequency for background subtraction and residence time studies. Both source chambers can be isolated from the rest of the vacuum system by O-ring slide valves positioned over the collimating holes in the source buffer chamber walls. In this fashion, the beam sources can be changed without venting the ultrahigh vacuum main chamber and detector.

The beam sources that have been employed to date are 0.003" diameter heatable stainless steel nozzle and a 0.040" diameter skimmer mounted via a bellows arrangement to the source flange and an effusive hydrogen atom source. The hydrogen atoms are produced with a 72% dissociation yield in a discharge sustained at the tip of the nozzle. As shown in Fig.3, a water cooled microwave cavity[4] is mounted on the end of an oil-cooled, double walled glass tube, the inner tube of which has a 1 mm orifice at its end. The pressure behind the orifice is 0.5-1 Torr. A well-tuned cavity will sustain a discharge with 60 W of power at 2450 Mhz.

Main Scattering Chamber

The main chamber is an 18"diameter Ultek bell jar with a 22" wire seal flange. This flange is the reference surface for the beam and detector alignment and divides the main chamber into a stationary section,

lengthened to 27.25", and a movable section. As shown in Fig.2, there are two major groupings of flanges on the stationary part of the main chamber. At the beam level there are six viewports covering 157°. This number of viewports allows laser light that is shined through the primary beam source (lower beam source in Fig.2) and reflected off the surface and through the detector to be viewed at many angles of incidence. This procedure for sample surface alignment ensures that the plane of the sample surface is perpendicular to the plane determined by the primary incident beam and the detector viewing angle. At a level 7.25" from beam level are flanges which accommodate retarding grid optics, an electron gun and an ion gun for performing LEED, AES, and sputtering. The detector chamber is mounted on the other section of the main chamber cylinder which is movable to gain access to the detector. The movable section of the main chamber accommodates the flanges which provide electrical, cooling, and motion feedthroughs for the detector chamber. The main chamber is pumped by a 400 l/sec noble ion pump, a titanium sublimator, and a 6" liquid-nitrogen trapped-diffusion pump which can be isolated from the main chamber by a metal sealed gate valve.

Detector Chamber

The detector chamber is enclosed entirely in the main chamber. Since the magnets of the 30 l/sec ion pumps which are employed as pumps on each of the two differential chambers are incompatible with ultrahigh vacuum, the detector chamber is double walled. The outer jacket houses the magnets and is connected to the atmosphere by a set of three flexible bellows. The detector chamber is cooled by circulating water through the outer jacket. This cooled surface area allows more efficient pumping of the titanium sublimators which are present in each of the differential chambers.

The detector chamber is supported and rotates on a ring mounted inside the movable section of the main chamber as shown in Fig.2. The rotational motion of the detector is provided by a linear and angular motion feedthrough. With the present slit arrangement, the angular resolution is 1.5°.

A cross-beam Pierce gun-type ionizer, UTI quadrupole rods and electronics, and a Channeltron electron multiplier comprise the mass spectrometer

detector. The flight path between the center of the ionizer of the mass spectrometer and the chopper wheel is about 12 cm. The chopper wheel is clamped on the shaft of a Globe 75A814 motor which is bolted onto the side of the detector chamber so that the scattered beam is modulated just before entering the first collimating slit, as shown in Fig.3. The 8" diameter titanium-aluminum alloy chopper wheel has a pseudo-random slit pattern machined into its periphery. The cross correlation technique for time-of-flight analysis is used primarily because of its large duty cycle (50%) compared to the single shot method (2%).[5] A light emitting diode and a photodiode receptor (Sharp GL514/PD 50PI) mounted around the chopper wheel produce a trigger signal for every revolution of the wheel.

Manipulator

The manipulator has four main parts. The xy carriage (Fig.4) which mounts the whole of the manipulator bolts directly onto the main chamber. The xy carriage has additional feedthroughs for providing a coolant to the sample surface. The secondary stage of the carriage moves vertically and supports the horizontal stage. The bottom flange (Fig.5) mounts directly onto the horizontal stage and provides an anchor for the three rods supporting the upper and intermediate flanges and for three threaded rods for translational motion. The top flange (Fig.5) provides the rotational and z translational degrees of freedom. The crystal holder assembly (Fig.7) is attached to the top flange by a 3/8" shaft. The intermediate flange (Fig.6) provides the rotational and translational motion of the tilt wedge for tilting the sample surface and the electrical feedthroughs.

The 7.25" translation of the sample surface occurs by movement of the top and intermediate flanges relative to the bottom flange. Rotary motion of one of the threaded rods is transferred to the other two by a sprocket and a chain arrangement near the bottom flange. A long stainless steel welded bellows is bolted to the intermediate and bottom flanges.

The incident angle of the beam with the sample surface is changed by rotating the entire sample surface holder assembly mounted on a Huntington rotary feedthrough. The rotary feedthrough has a coaxial linear motion capability which enables the azimuthal angle of the sample surface to be varied (rotation of the sample surface around a line perpendicular to

its plane). The ceramic sample surface mount shown in Fig.7 is rotated by pulling a thin wire which is wrapped around and anchored to the ceramic. Upon releasing the wire, the ceramic mount rotates backwards by the tension provided by a small clock spring. The ceramic mount is press-fit into a small bearing. The wire is attached to the 1/8" rod which is coaxial with the 3/8" shaft of the rotary feedthrough. The azimuthal angle can be varied $\pm$ 180°.

The sample surface holder is manufactured from two parts - the stem and the spherical surface which have been brazed together. The sample surface sits in the stem at the center of a sphere of which the spherical surface is a section. The spherical section is spring clamped between two spherical surfaces, the upper and lower tilt surfaces. Movement of the spherical surface with respect to the upper and lower tilt surface causes the tilt of the sample surface around its center. The angular tilt is limited to $\pm$ 6°. The movement of the spherical surface is effected by translating the tilt wedge to touch the circumference of the spherical section. As translation of the wedge is increased, the spherical section and the sample surface tilt because of the shape of the tilt wedge. The tile wedge is translated by motion of the intermediate flange relative to the top and bottom flanges. A short bellows with 1" of travel is bolted between the top and intermediate flanges. The tilt wedge is rotated to any angle around the spherical section by a rotary feedthrough on the intermediate flange coupled by a gear to the tilt tube.

The intermediate flange accommodates seven electrical feedthroughs at the end of which Be-Cu prongs are bolted. These prongs form a spring contact with copper rings stacked between alumina spacers. Each ring is attached to a copper wire which runs down through the tilt tube to the crystal. The copper rings and leads rotate with the tilt tube relative to the stationary prongs. This rotatable electrical contact avoids long troublesome flexible leads to the crystal. Only the last 1.5" of the leads are flexible copper braid. As many as 3 amps have been passed through the rotatable spring contacts. The sample surface is heated by electron bombardment.

Signal Electronics

The 10-15 mV pulses out of the Channeltron are passed through a pre-amplifier, discriminator, and a pulse shaper. In the angular distribution mode, the output pulses are fed into two counters gated by a timer gater module LBL13x3050. The module outputs two gates whose phase and width are set to maximize the difference in counting rates between the two counters. The timer gater module is triggered from a pick-up coil of a 150 hz tuning fork chopper mounted in the buffer chamber of one of the beams. Thus one counter corresponds to the signal plus background and the other to the background signal when the chopper is closed. The timer gater module counts for a preset amount of time.

In the velocity analysis mode, the output pulses from the amplifier are fed into a 255 multi-channel scalar, LBL13x3501-P1. The multi-channel scalar is triggered to start the address advance by the trigger pulses from the LED/photodiode pair once every revolution of the copper wheel. The multi-channel scalar advances the addresses and also puts out a motor synch pulse every dwell time to externally drive the motor driver oscillator. The multi-channel scalar is interfaced to a Nova 2-10 computer via a Camac crate and controller. An oscilloscope display is also interfaced to the computer via a point plotter in the Camac crate. A program controls the acquisition of the data and performs the deconvolution of it.

Results

The oxidation of deuterium on a Pt(111) surface has been studied and samples of the results are presented here. Deuterium is the gas in the primary source and is modulated in the angular distribution measurements. Oxygen is placed in the secondary source. The angular distributions of the D_2O product from the reactions D_2+O_2 and $D+O_2$ reactions are shown in Figures 8 and 9. The error bars represent two standard deviations. Figure 10 presents a D_2O product time-of-flight distribution for the case of the molecular reactants. The signal counting rate is 20 c/sec with a 1200 c/sec background count. This small counting rate indicates that for every 10^3-10^4 D_2 or O_2 molecules incident on the surface, one D_2O molecule

is formed. This small reaction probability and broad angular distribution underscores the need for close and intense incident beams and differential pumping of the detector. It is calculated that the background count would be at least one order of magnitude higher if the mass spectrometer were placed in the main chamber. It is desirable to increase the total counting rate since the time required to achieve a given signal to noise decreases in proportion to an increase in the counting rate for signals much smaller than the background. The total counting rate can be increased by improving the mass spectrometer detector efficiency through additional quadrupole lensing on the ionizer and higher RF frequency on the quadrupole rods which will increase the sensitivity of the mass filter for low mass numbers.

Acknowledgements

This work was supported by the Director, Office of Energy Research, Office of Basic Energy Sciences, Materials Sciences Division of the U.S. Department of Energy under Contract No. W-7405-ENG-48, and the National Science Foundation. Discussion with Y.T. Lee are gratefully acknowledged.

References

1. S.T. Ceyer, Ph.D. Thesis, University of Calfiornia, Berkeley, 1979.
2. R. Calder, G. Lewin, Brit. J. Appl. Phys. 18, 1459 (1967).
3. C.T. Foxon, M.R. Boudry, B.A. Joyce, Surface Sci. 44, 93 (1974).
4. F.C. Fehsenfeld, K.M. Evenson, H.P. Broida, Rev. Sci. Instr. 36, 294 (1965).
5. V.L. Hirschy, J.P. Aldridge, Rev. Sci. Instr. 42, 381 (1971).

Figure Captions

Figure 1. a) Surface residence time experiment. b) Time-of-flight experiment.

Figure 2. Schematic assembly drawing.

Figure 3. Assembly cross section through scattering leve. (A) Primary source flange, (B) Window, (C) Blank flange, (D) Ion gauge, (E) Chopper motor, (F) Ring, (G) Mass spectrometer, (H) Motor water cooling lines, (I) Primary source chamber, (J) Primary buffer chamber, (K) Ion gauge, roughing port, (L) Right angle pneumatic valve, (M) LN trap, (N), Gate valve, (O) Detector chamber, (P) Bearing mounting block, (Q) Main chamber ion pump, (R) Main chamber titanium sublimator, (S) Rotation drive mechanism.

Figure 4. Side view and cross section of xy carriage. (A) Rectangular plate stationary stage, (B) Secondary stage or vertical slide rods, LC) Primary stage handle, (D) Primary stage or horizontal slide rods, (E) Primary stage, (F) Secondary stage handle, (G) Secondary stage, (H) Miniconflat flange.

Figure 5. Cross section of bottom flange and tilt tube support. (A) 3/4" support rod, (B) bottom flange, (C) tilt tube support, (D(tilt tube support bearing, (E) 5/8" threaded rod, (F) Sprocket and chain for z translation drive, (G) bellows.

Figure 6. Assembly of top and intermediate flanges. (A) Rotary motion feedthrough for angle of incidence rotation, (B) Micrometer, (C) Threaded rods for z translation, (D) Sprocket chain and threaded rods for tilt wedge translation, (E) Top flange, (F) $4^{4^{\circ}}$ threaded rods and nuts, (G) Ceramic disk spacers, (H) Gear on rotary feedthrough, (I) Rotary feedthrough for tilt wedge rotation, (J) Tilt tube holder, (K) Tilt Tube, (L) 3/8" shaft, (M) 1/8" rod, (N) 1/16" electrical wife, (O) Tilt tube gear, (P) 1/8" Plate, (Q) Be-Cu bushing, (R) Intermediate flange, (S) Electrical feedthrough flange, (T) Copper ring.

Figure 7. Assembly cross section of sample surface holder, tilt wedge and tilt tube. (A) Tilt tube, (B) 1/8" SS balls, LC) 3/8" shaft, (D) Ceramic rings, (E) 1/16" Cu wire, (F) 1/8" azimuthal drive rod, (G) Spring, (H) Tilt wedge, (I) Roller assembly and 0.005" wire, (J) Ceramic crystal mount, (K) Clock spring, (L) Ceramic filament holder, (M) Lower tilt surface, (N) Crystal holder, (O) Upper tilt surface, (P) Set screw, (Q) 3/8" shaft bearing and metal spacer for electrical wires.

Figure 8. D_2O product angular distribution at T_s = 698 K.

Figure 9. D_2O product angular distribution at T_s = 698 K.

Figure 10. D_2O product time-of-flight spectrum at T_s = 913 K and θ= 7.7°. Total counting time - 9 hours.

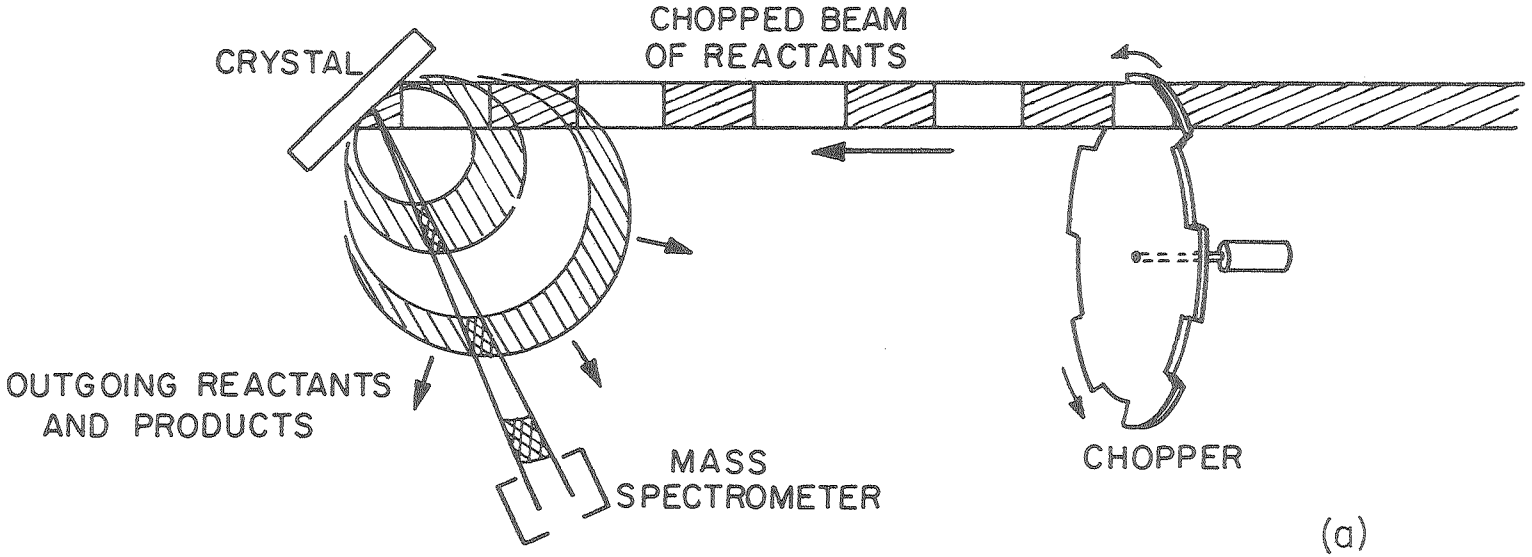

(a)

XBL 812-8098

Fig. 1a

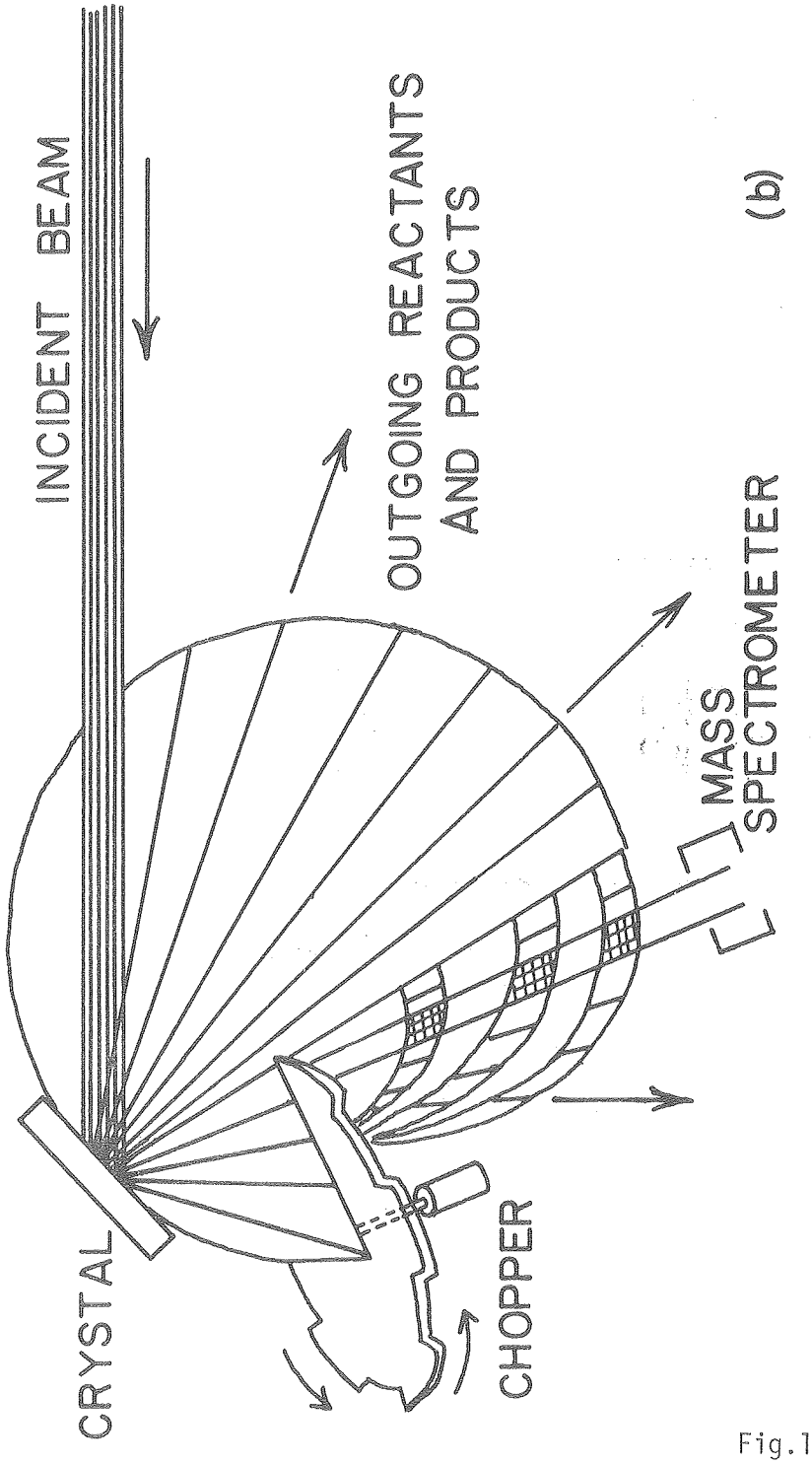
INCIDENT BEAM
OUTGOING REACTANTS AND PRODUCTS
MASS SPECTROMETER
CRYSTAL
CHOPPER
(b)
XBL 812-8100

Fig.1b

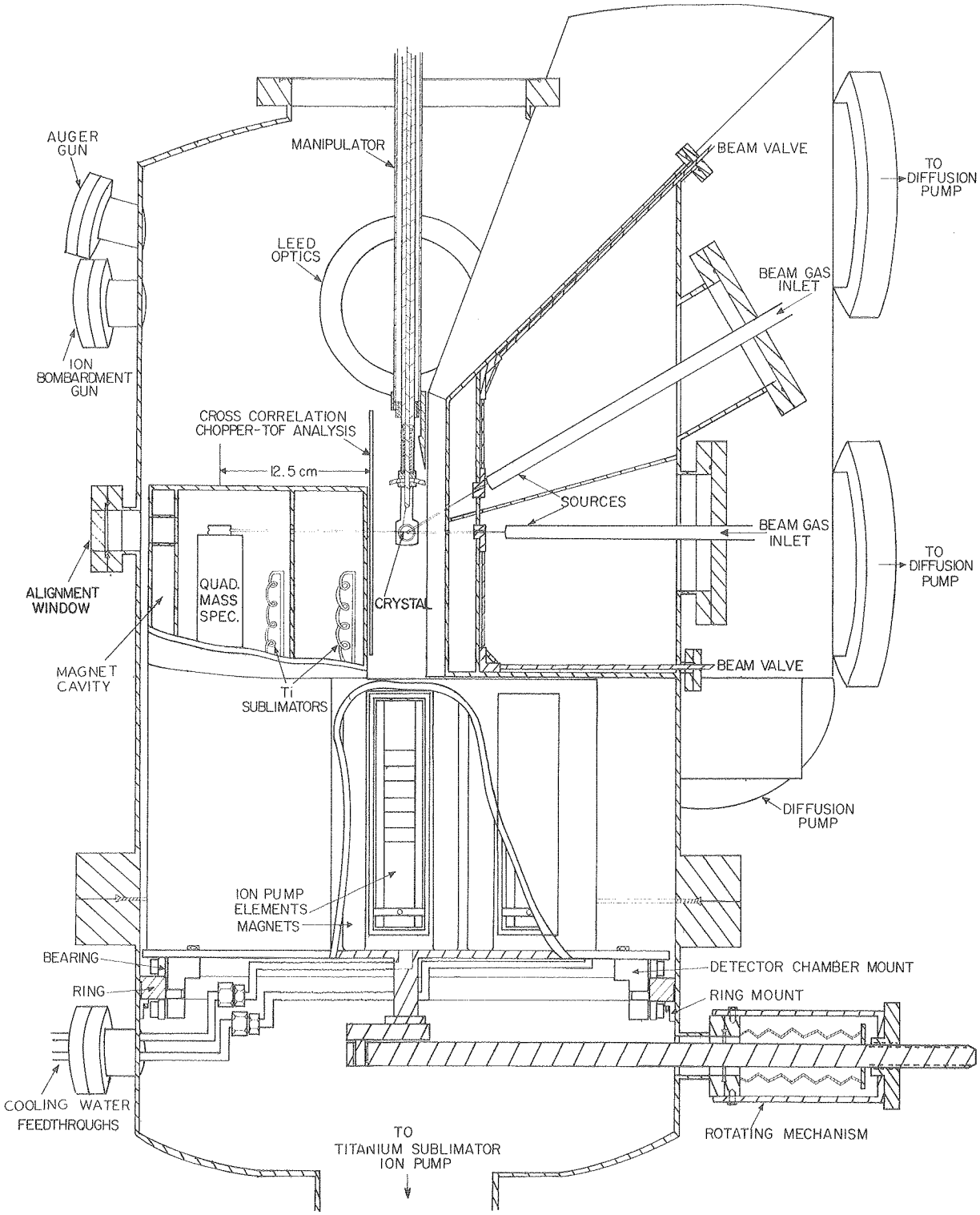
AUGER GUN
MANIPULATOR
BEAM VALVE
TO DIFFUSION PUMP
LEED OPTICS
BEAM GAS INLET
ION BOMBARDMENT GUN
CROSS CORRELATION CHOPPER-TOF ANALYSIS
12.5 cm
SOURCES
BEAM GAS INLET
TO DIFFUSION PUMP
ALIGNMENT WINDOW
QUAD. MASS SPEC.
CRYSTAL
BEAM VALVE
MAGNET CAVITY
Ti SUBLIMATORS
DIFFUSION PUMP
ION PUMP ELEMENTS
MAGNETS
BEARING
DETECTOR CHAMBER MOUNT
RING
RING MOUNT
COOLING WATER FEEDTHROUGHS
TO TITANIUM SUBLIMATOR ION PUMP
ROTATING MECHANISM
XBL 799-11376

Fig.2

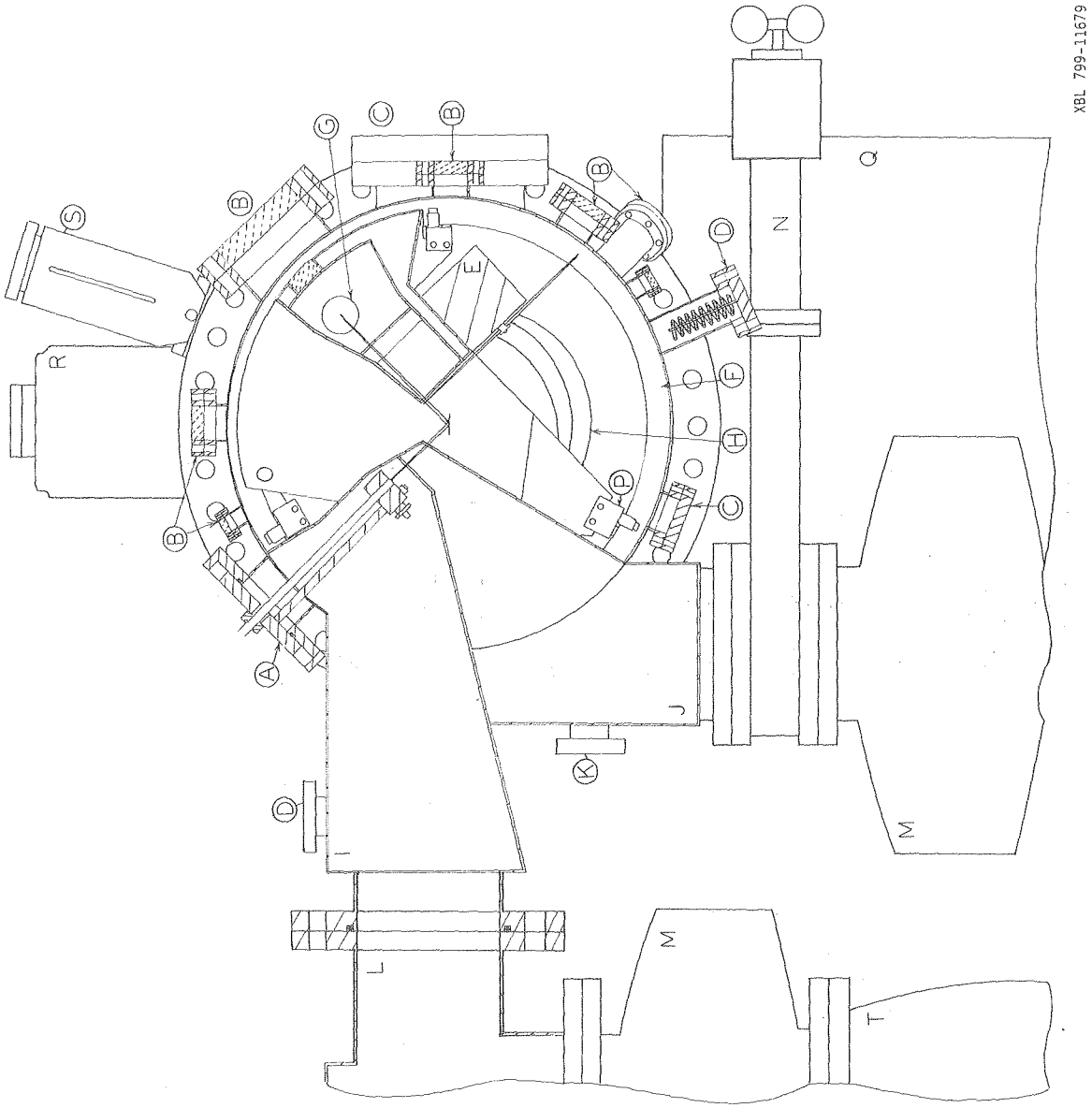

Fig.3

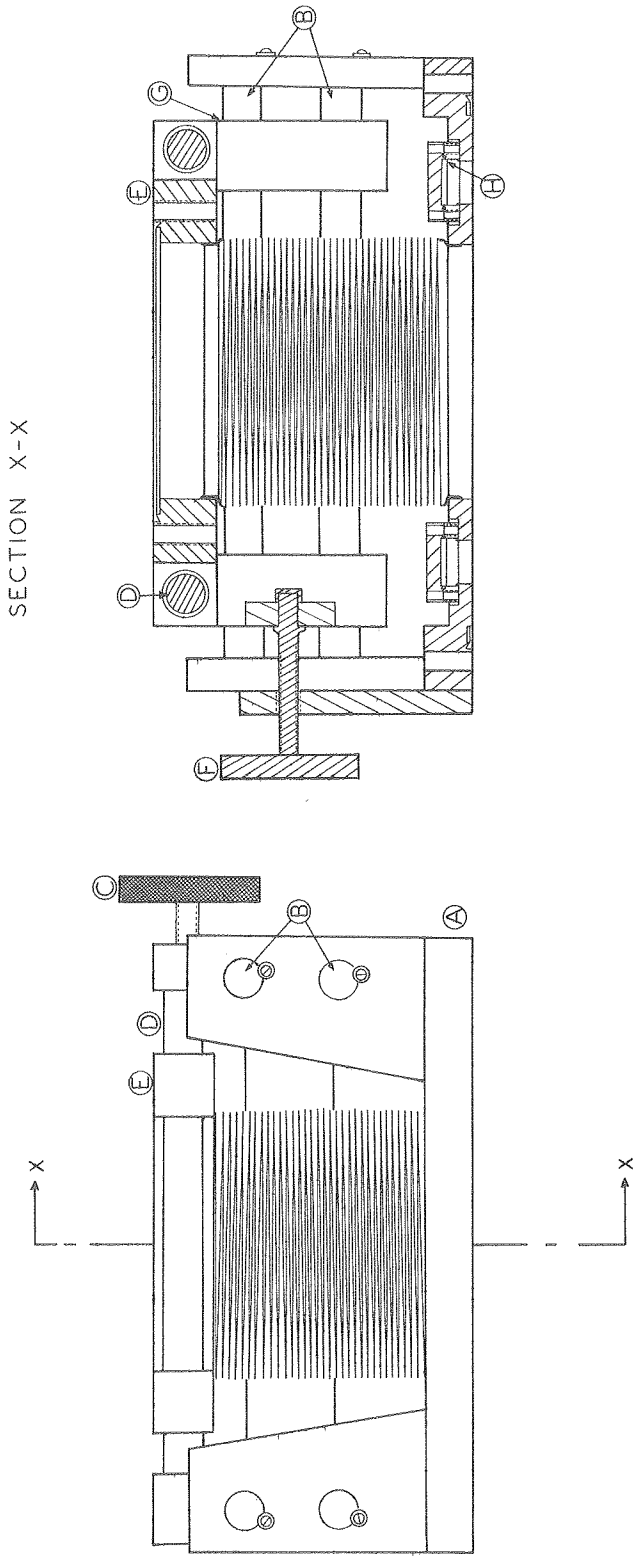

XBL 799-11375

Fig.4

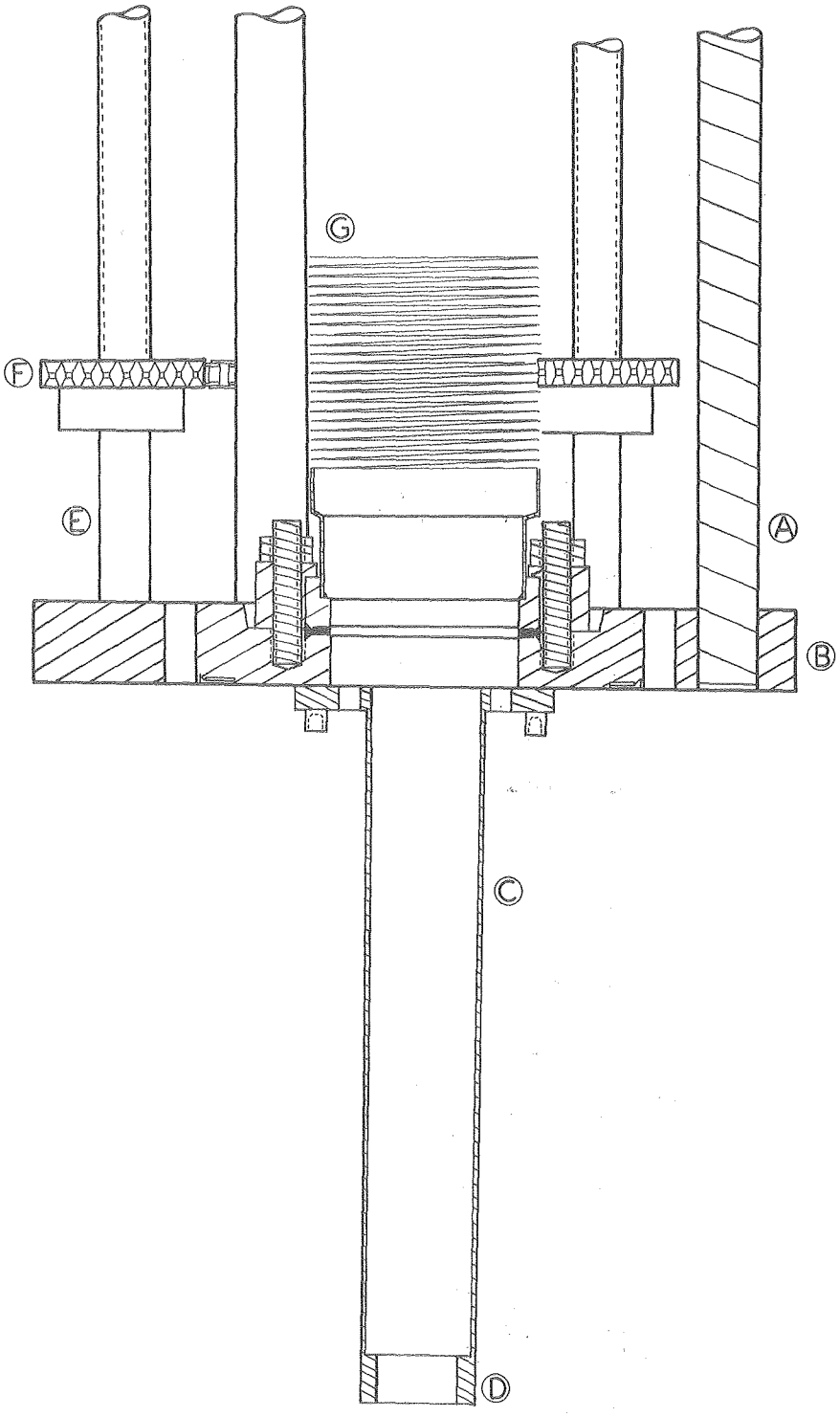

XBL 799-11381

Fig.5

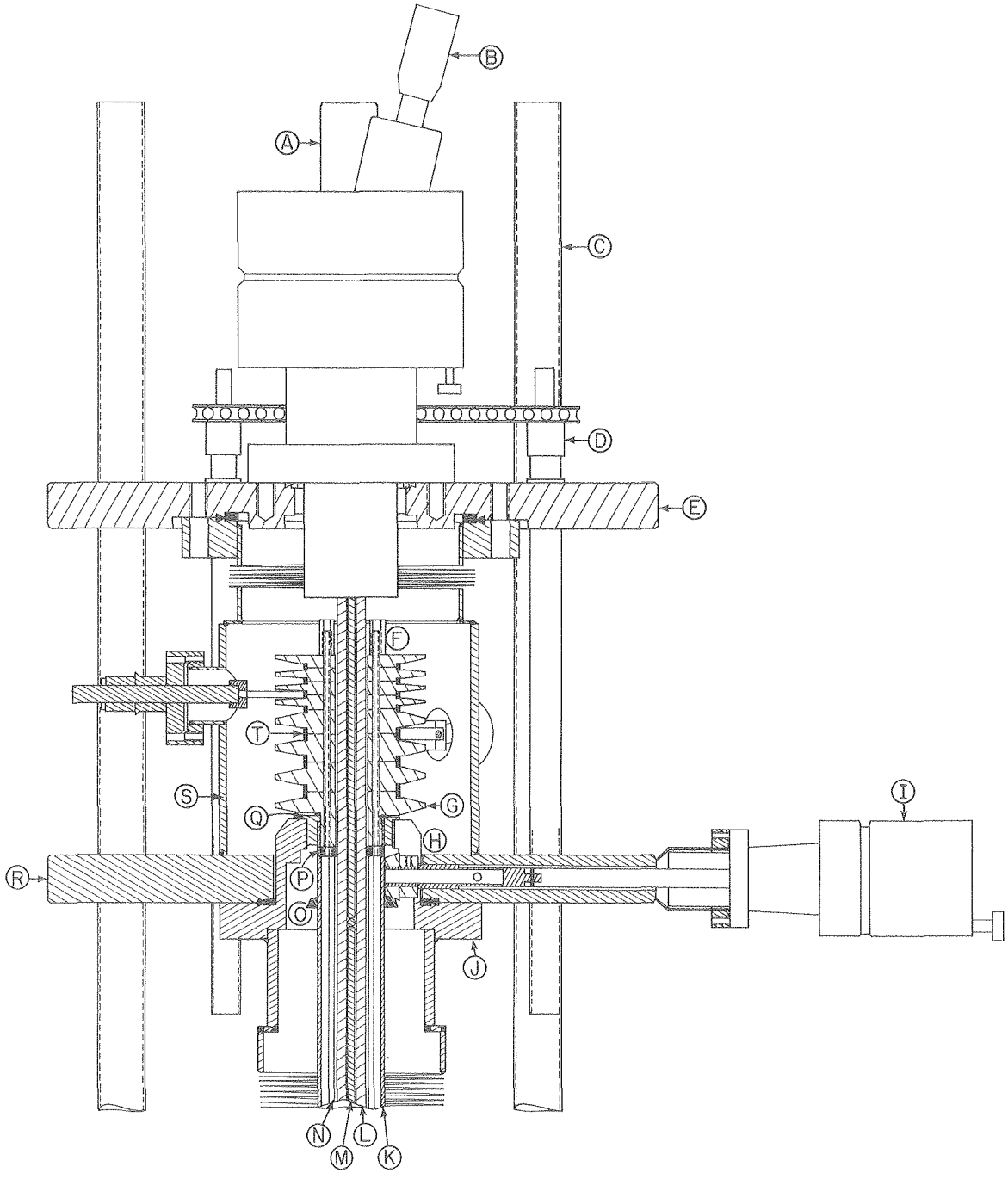

Fig.6

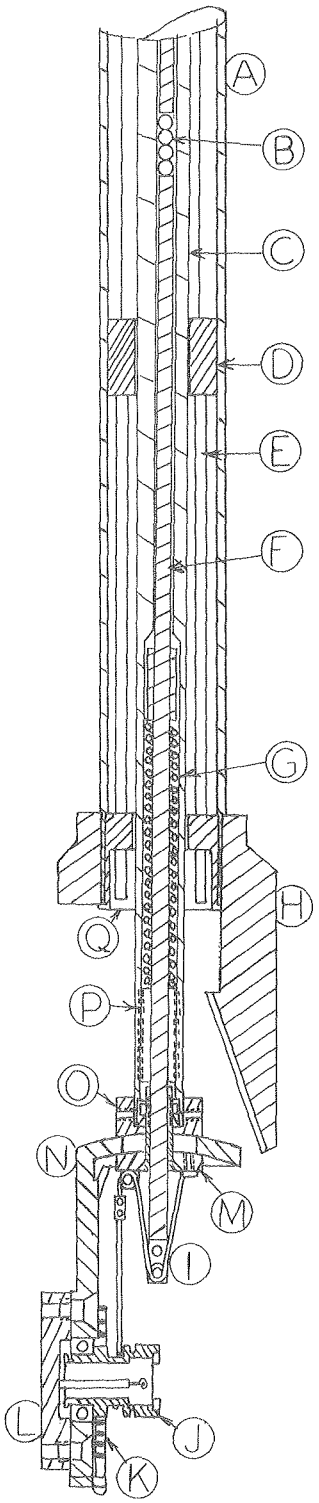

XBL 799-11380

Fig.7

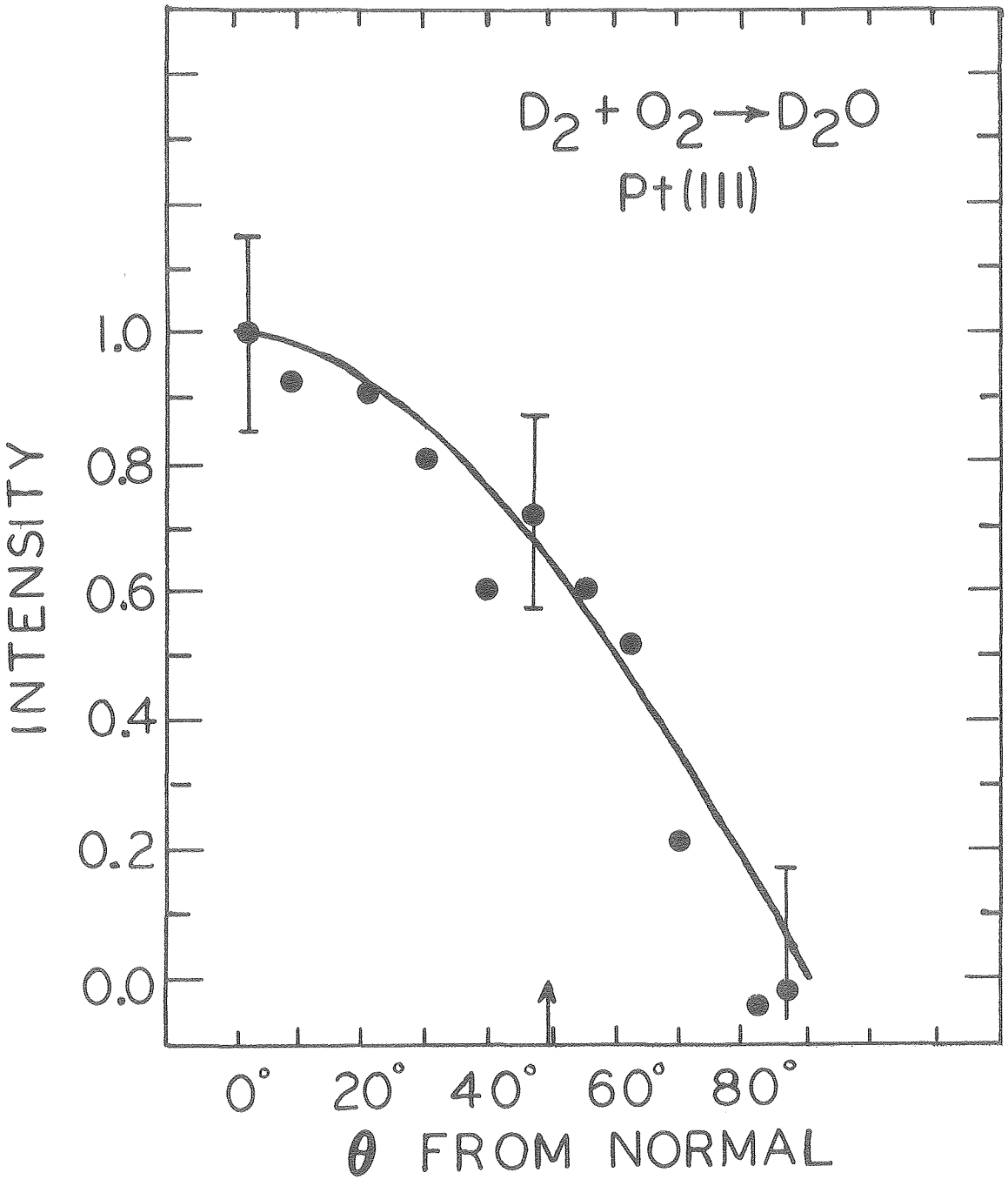

XBL 799-11675

Fig.8

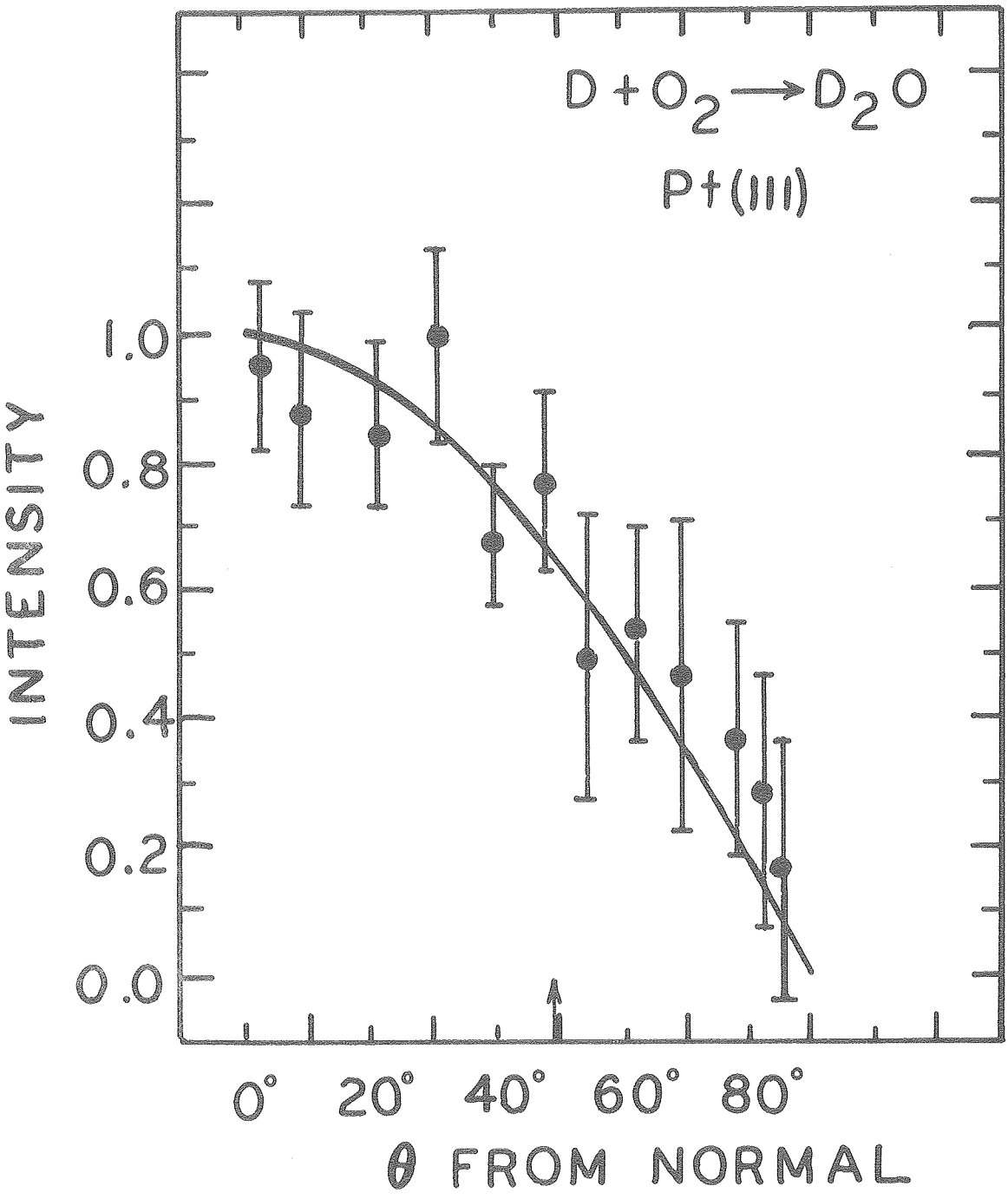

XBL 799-11676

Fig.9

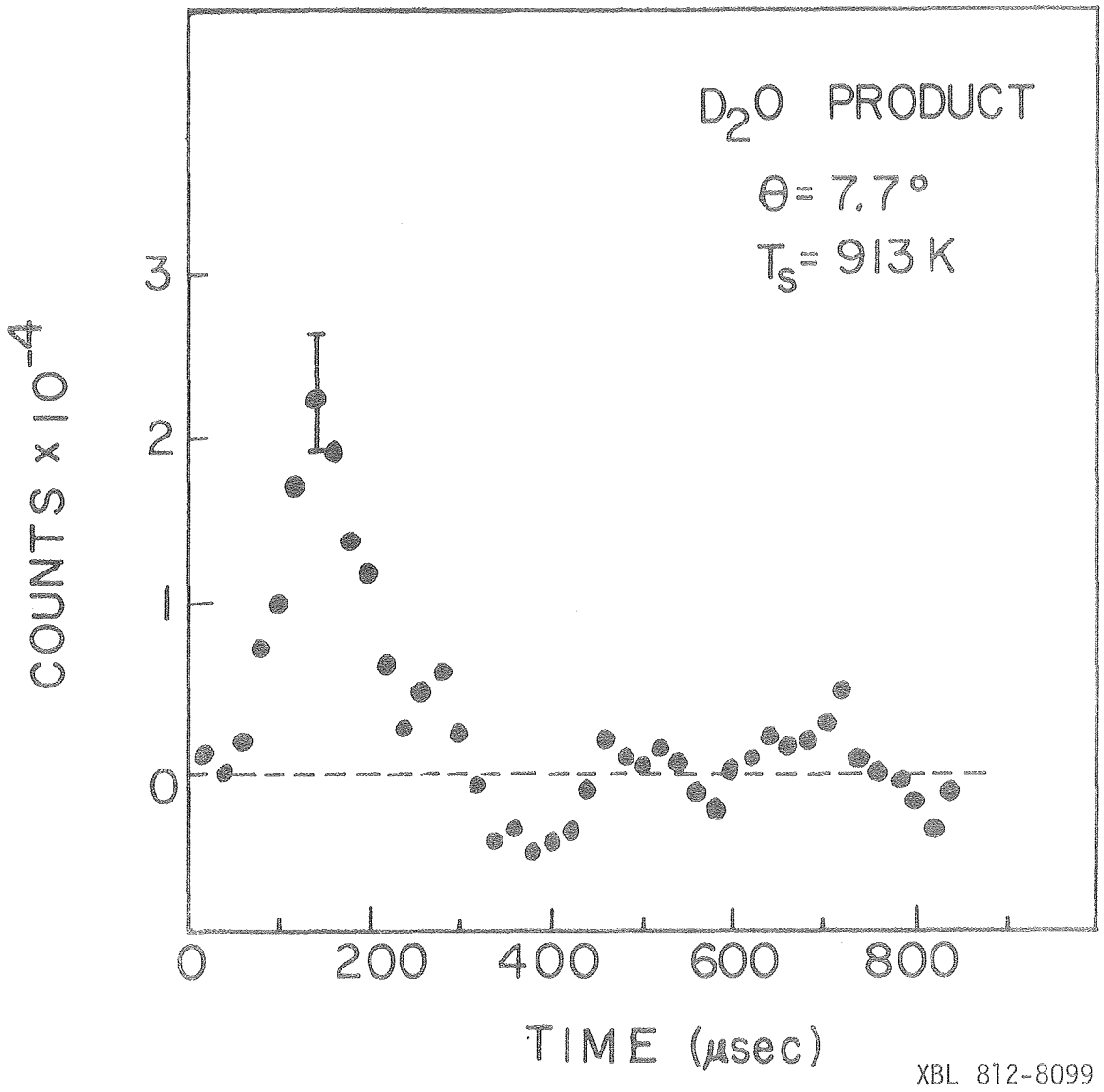
D_2O PRODUCT
θ = 7.7°
T_s = 913 K
COUNTS x 10^{-4}
3
2
1
0
0
200
400
600
800
TIME (μsec)
XBL 812-8099

Fig.10